

Appearance of images through a multifocal intraocular lens

Eli Peli

The Schepens Eye Research Institute, Harvard Medical School, 20 Staniford Street, Boston, Massachusetts 02114

Alan Lang

Allergan Surgical VK-1D, 2525 Dupont Drive, Irvine, California 92623-9534

Received July 21, 2000; revised manuscript received September 28, 2000; accepted October 2, 2000

The appearance of images through a multifocal intraocular lens (IOL) was simulated. The optical transfer function (OTF) of a model eye containing the multifocal lens was measured and divided by the OTF of the model eye with a monofocal IOL. This ratio was used to filter digital images, generating simulations that represent the retinal images seen through a multifocal intraocular lens when viewed through an eye with a monofocal lens. A dichoptic side-by-side display was used to present the original image to one eye, implanted with the multifocal lens, while the other eye, implanted with monofocal lens, viewed the simulations and variations on the simulations to derive a point of subjective equivalence. Four subjects with such bilateral lens implants were tested for near and distance vision. The results validate the test methodology and the simulations. Referenced to the nominal theoretical filter, the prediction was within a 0.25-diopter (D) blur for distance simulation and within a 0.50-D blur for the near-vision simulation. © 2001 Optical Society of America
OCIS codes: 330.4060, 330.5510, 330.6100, 330.6110, 330.7310.

1. INTRODUCTION

Multifocal intraocular lenses (IOL's) of various designs are now used to replace the eye's crystalline lens in cataract surgery.¹⁻³ To enhance near vision, which is not done by monofocal IOL's, the multifocal IOL simultaneously images near and far points on the retina. Thus at every viewing distance an out-of-focus image is simultaneously added to the clear in-focus image. The nature and quality of the vision provided by such lenses is important. While positive subjective responses were found in clinical trials leading to the approval of these lenses,¹ it is of interest to be able to simulate the vision with such lenses to observers with normal sight. If validated, such a simulation can be used as a design tool in developing better or different lenses.

Pictorial representations of image appearance using the visual system's modulation transfer function (MTF) have been attempted by various investigators over the years in a variety of applications in vision science and engineering.⁴⁻⁹ The use of the MTF in simulations assumes that the optical system introduces no changes in phase. This may be incorrect when the optics of a blurring (out-of-focus) lens is involved. In such cases the more complete description of the system, the optical transfer function (OTF), is necessary to represent the polarity reversals that may occur. The MTF and OTF of eyes with such multifocal IOL's have been measured and computed.^{10,11} It is generally believed that the OTF provides all the information needed for determination of image appearance and image quality. Although the OTF should be sufficient to determine the *retinal* image accurately, it cannot predict perception directly because of the nonlinear nature of the visual system (threshold

response).^{6,12,13} However, in the unusual situation of the comparison of the image appearance between two eyes of the same person, one equipped with a monofocal IOL and one with a multifocal IOL, the between-eyes' OTF ratio will properly describe the difference between the retinal image in the multifocal IOL and the retinal image in the monofocal IOL. Using linear Fourier optics, the retinal image $[\text{Ret}(\bar{x})]$ is proportional to the inverse Fourier transform of the product of the OTF of the eye multiplied by the Fourier transform of the object $[\text{object}(\bar{x})]$:

$$\text{Ret}(\bar{x}) = C(F^{-1}\{\text{OTF}(\bar{k})F[\text{object}(\bar{x})]\}), \quad (1)$$

where C is a normalization constant, $F[\cdot]$ is the Fourier transform, and \bar{k} is the spatial frequency. This expression should hold for either eye. If the monofocal eye perceives the same image as the multifocal eye, then the retinal images are equal. Given this equivalence of retinal images, the object presented to the monofocal eye (the filtered image) should be:

$$\text{Filtered image}(\bar{x}) = F^{-1}\left\{\frac{\text{OTF}_{\text{multifocal eye}}}{\text{OTF}_{\text{monofocal eye}}}F[\text{object}(\bar{x})]\right\}. \quad (2)$$

Thus the image appearance based on the OTF can be tested directly in such patients and can be used to verify the OTF. Under the assumptions that the OTF of the eye with a clear crystalline lens does not differ much from the OTF of the eye with a monofocal IOL and that the visual processing is the same for the two eyes (e.g., not amblyopic), the same simulations can represent the appearance to any observer with clear optical media.

We conducted experiments to test the simulations for both distance and near vision using an approximation of

the OTF based on measurements of line-spread functions. OTF ratios were used to computationally modify images to simulate their appearance through the multifocal IOL and present them to the monofocal IOL eye. If the OTF and the resulting simulations were valid, the simulated image seen through a monofocal IOL should be indistinguishable from the original (standard) image seen through the multifocal IOL.

2. METHODS

A. General Method

Four subjects participated in the study: one man and three women, ages 68–77 years. All four had a multifocal IOL (ARRAY[®], Allergan) in one eye and a monofocal IOL (SI26NB, Allergan) in the other.

The ARRAY multifocal IOL consists of five annular refractive zones, alternating primarily between the power for distance and the near reading addition (ADD) power equal to the distance power plus 3.5 diopters (D).¹ This ADD power is effectively equivalent to approximately a +2.7-D presbyopic spectacle ADD, which allows reading at approximately 37 cm. The center zone is distance-correction dominated to maintain sharp distance vision in bright sunlight conditions. The surface curvature transitions between zones are designed to direct all light rays somewhere between these two main refractive powers, thereby enhancing the range of usable intermediate distance vision. The zone radii are chosen to minimize the variations in the percentages of light directed to distance, intermediate and near, as the pupil size varies in this older, cataract-age population.

Pretest examination, in addition to slit lamp evaluation, included measurements of visual acuity at distance (20 ft), sighting dominance, stereoacuity at distance, and suppression tests with use of a computerized vision testing device, the BVAT (Mentor O&O). Subjective refraction was determined by using a standard clinical procedure and was used to modify the subject's spectacle correction when needed.

Stereo ferro-electric liquid-crystal (LC) shutter goggles allowed presentation of different images to each eye (dichoptic). Both images were visible side by side, and the standard indicated which image was clearer (Fig. 1). The standard (unprocessed) image was always presented to the eye with the multifocal lens. The standard image was displayed on either the right or the left half of the screen but was seen only with the multifocal IOL eye.

Lenses placed in front of the eye were used to adjust for the subject's refractive error and to set the optical distance of the image as needed. The monofocal IOL eye was presented with a computationally modified version of the image on the other half of the screen (Fig. 1). A set of seven simulated images were presented for each scene (described in the image-processing section below), ranging from more blurred than the image simulating the view with the multifocal IOL eye. Each simulation of each scene was presented to the subject 10 times (70 trials per image). The order of scene and simulations presentations was randomized.

B. Optical Transfer Function Measurements

The OTF's of the multifocal and the monofocal IOL's (20 diopters) were recorded with a model eye composed of a wet cell containing the IOL. The model eye included an

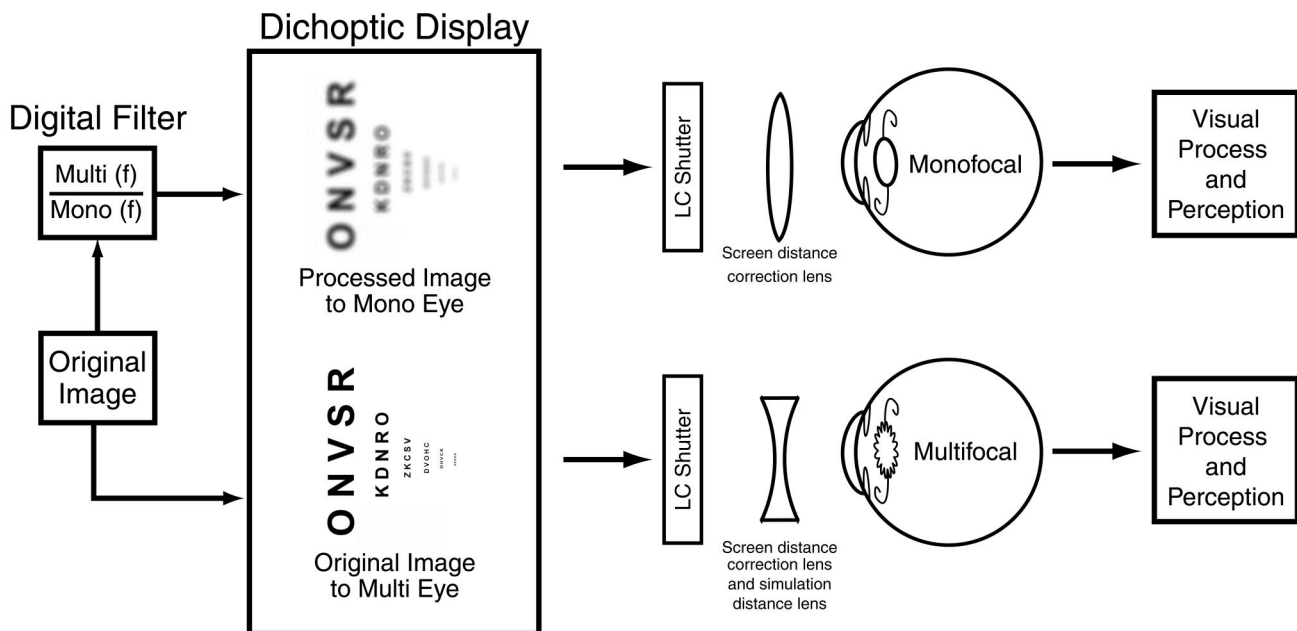


Fig. 1. Schematic illustration of the system used in the study. The original image was presented, through the LC shutters, only to the eye with the multifocal IOL (it could be presented on either the right or the left of the screen). The image presented to the eye with the monofocal IOL was filtered digitally. The filter was a ratio of the OTF's of the schematic eye with the multifocal IOL to the OTF's of the eye with a monofocal IOL. The various filters used are shown in Figs. 4 and 5. The monofocal eye was corrected with a lens for the screen distance. The multifocal IOL was either corrected for the screen distance (distance test) or presented with a total vergence of -2.75 D by using the combination of the distance and a negative lens. Assuming that the visual processing in each eye is equal implies apparent equality of perception when the digital filter correctly represents the ratio of the eyes' OTF's.

achromatic lens (36-mm focal length) used as the cornea and a 3-mm aperture and was configured to give the same retinal image height as the human eye.¹⁴ A broadband light source filtered to match the weighting of the photopic retinal response was used as a target. OTF's were measured with the EROS system (Ealing Electro Optics, U.K., now supported by Optikos, Boston, Mass.).

The EROS system calculates the one-dimensional OTF by Fourier methods applied to the image of a 2- μm -wide linear slit (line-spread function). A white light source, photopic filter, and collimating lens project the 2- μm target to infinity. The collimated beam enters the model eye ($F/8.2$, $f_l = 24.5$ mm) and creates an image in air. The image is collected by a 0.28-N.A. microscope objective and recorded by a linear diode array. Software performs the necessary calculations, displaying both the modulation

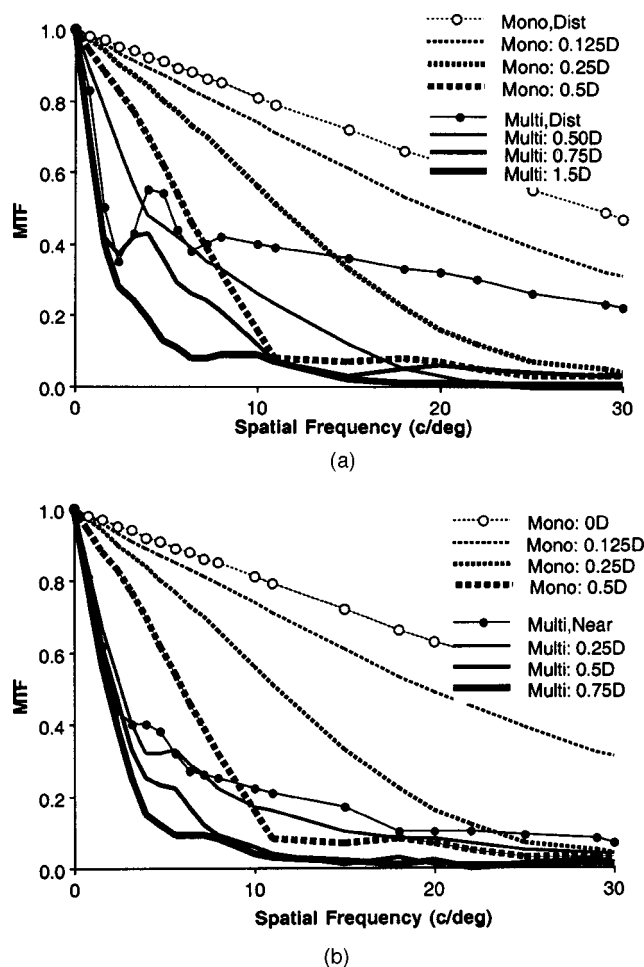


Fig. 2. The measured MTF obtained for the schematic eye with a multifocal IOL (solid curves) and with a monofocal IOL (dashed curves). (a) The MTF's with a multifocal lens for a distance (collimated) target (solid curve with dots), as well as additional MTF's obtained at different levels of blur (solid curves). (b) The MTF's with a multifocal IOL for a near (-2.75 -D vergence) target (solid curve with dots) as well as additional MTF's obtained at different levels of blur (solid curves). In both graphs the measured MTF's obtained for the schematic eye with a monofocal IOL (dashed curves) are illustrated for a distance (collimated) target (dashed curve with circles) as well as additional MTF's obtained at different levels of blur. The various blur levels MTF's were used for the various filter designs illustrated in Figs. 4 and 5.

transfer function (MTF) and the phase transfer function (PTF). The image of the slit at the distance conjugate is composed of a sharply peaked in-focus image formed by the distance power of the multifocal IOL plus an out-of-focus broad tail (skirt) due to the near out-of-focus component of the multifocal design. Care was taken to record the full image tail, without which the calculated amplitude of OTF is unrealistically high. Optical testing was performed on the optical axis of the schematic eye.

Experience with optical bench testing confirms the theoretical expectation that for axially symmetric optical systems, the PTF function is essentially flat or linear, except for 180-deg phase transitions where the MTF crosses zero. A linear PTF introduces a prismatic-like shift in the image as a result of some very slight misalignment of the optical components and has no significant effect on the overall image quality. Since the exact decentration of the IOL's in the subjects' eyes was not known and the image shift has no effect on perceived image quality, the linear phase was not used. No phase reversals were found or expected for the OTF computed for the multifocal IOL at either distance focus or near focus or for monofocal IOL at distance focus. Thus the measured phase had no impact on the computation of the corresponding filters and simulations. It should be noted, however, that in other cases, for example, in applying the same analysis to the simulation of a retinal image with a monofocal lens under the high level of blur that occurs at reading distance, the effect of these phase reversals could be substantial and should not be ignored.

In addition to measuring the OTF of the IOL at the best focus (peak line-spread function), the OTF under various defocus conditions was measured for both lenses (Fig. 2). Defocus monofocal and multifocal OTF's were created by changing the back focal position by the amount calculated to be equivalent to the spectacle defocus specified. OTF's with phase reversals occurred in only the most defocused conditions. These extreme OTF's created filters for the sharpest and blurriest images, which in our paradigm had minimal effect on the results. Further, note that the existence of zeros in the OTF of the monofocal IOL will cause difficulties in Eq. (2) in general. Since the application of this equation was discrete and at low resolution, we did not have to address this difficulty in our approximation even for the few cases where it might have occurred.

The EROS system computes only 17 points for each OTF file. The range of frequencies for which this sampling is applied was modified in various testing conditions. Because of the limited sampling of the OTF's, interpolated values were used in the construction of the filters where needed. After data collection, we realized that the sampling for the multifocal OTF under $+0.5$ -D blur condition was insufficient at the low frequencies, resulting in the loss of the low-frequency ringing pattern seen in the in-focus multifocal distance OTF. The results for this filter were not used in the analysis.

C. Image Processing

Four different color scene images were used (Fig. 3). The two scenes used for distance vision testing depicted a Roman temple and sailboats on a lake. The scenes used for



O N V S R

K D N R O

Z K C S V

D V O H C

O H V C K

H Z C K O

Fig. 3. The four scenes used in the testing. The two images on top, Temple and Boats, were used for distance vision simulation and testing. The two images on the bottom, Holly and Chart, were used for near-vision testing at a nominal optical distance of 36 cm. Color images were used in the actual simulations and testing.

the near-point testing depicted a Holly plant and a letter visual acuity chart (0.1 log steps for smaller letters and 0.2–0.3 for larger letters).

At the viewing distance of 135 cm used, the 20-cm-square, 512×512 -pixel image represented a maximum spatial frequency of 30 cycles/deg. A +0.75-D correction was used in front of the eyes as appropriate to compensate for this viewing distance.

Images were processed with software written in Microsoft Visual Basic. The filters computed from the ratios of the various (one-dimensional) OTF's (Figs. 4 and 5) were used to create the two-dimensional filters as rotationally symmetric filters in the spatial frequency do-

main. Since the final images were displayed on a Gamma-corrected system, the filtering was applied to each of the RGB components separately.¹⁵ Each color plane was transformed to the Fourier domain by a fast Fourier transform (FFT), was multiplied by the appropriate filter, and was transformed back to the space domain by an inverse FFT; e.g., Eq. (2).

Following filtration, the simulated image (originally 256 levels for each color) was compressed to 254 optimally selected colors to permit display in a pcx image format on the Vision Works¹⁶ system. Visual inspection demonstrated that the compressed images were indistinguishable from the originals.

D. Simulation and Presentation of Multifocal Near Images

The ratio of the multifocal near OTF to the monofocal distance (in-focus) OTF was used to create the simulated image (marked 0.0 D in Fig. 4). This image seen in focus through a monofocal IOL represents our prediction of the retinal image seen through the multifocal IOL at the nominal reading distance.

To obtain more-blurred images, the multifocal near OTF was measured at three additional levels of spectacle defocus (+0.25 D, +0.5 D and +0.75 D), and the corresponding OTF ratios were computed by dividing the various multifocal OTF's by the monofocal distance OTF point by point. In retrospect, the use of minus spectacle defocus would have been preferred (for the near-images case), because with the plus lenses the defocus moved toward

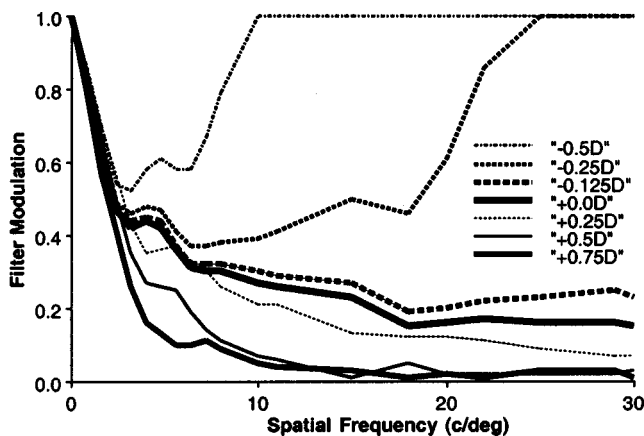


Fig. 4. The OTF ratios used to simulate the appearance of images from a near viewing distance. The predicted ratio (marked 0.0 D) was computed by dividing the OTF of the multifocal IOL, measured in a schematic eye from the near distance by the OTF of a best-corrected monofocal IOL. Blurrier images were obtained by measuring the OTF of the multifocal lens at different levels of blur (+0.25, +0.50, +0.75 D) while sharper images were obtained by blurring (-0.125, -0.25, -0.5 D) the monofocal IOL.

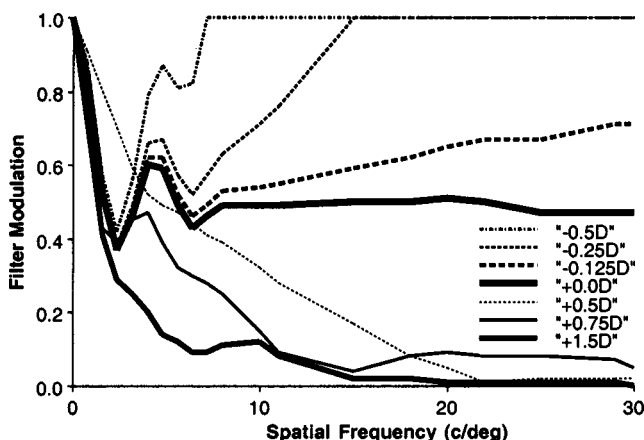


Fig. 5. The OTF ratios (filters) used to simulate the appearance of images from a distance. The predicted ratio (marked 0.0 D) was computed by dividing the OTF of the multifocal IOL, measured in a schematic eye from a distance, by the OTF of a monofocal IOL in the same eye from the same distance. Blurrier images were obtained by measuring the OTF of the multifocal IOL at different levels of blur (+0.50, +0.75, +1.50 D), and sharper images were obtained by blurring (-0.125, -0.25, -0.5 D) the monofocal IOL.

the distance focus. Nevertheless, the through-focus response for the ARRAY shows a clear monotonic decrease in MTF at intermediate distance,¹⁷ as required for this experiment; see Fig. 2 for the defocused multifocal near MTF's.

To obtain the sharper set of images, the monofocal distance OTF was measured at three levels of spectacle defocus (-0.125 D, -0.25 D, and -0.5 D), and the corresponding OTF ratios were computed by dividing the multifocal near OTF by the various monofocal defocus levels. The ratios and the corresponding filtered images are labeled as the corresponding defocus levels in Fig. 4.

The subjects viewed the original unfiltered image through the multifocal IOL using the ADD power provided by the multifocal IOL (2.75-D nominal ADD) and a trial lens correcting for the actual viewing distance. This was achieved by adding a -2.00-D lens to the 0.75-D vergence for the actual distance. The -2.00-D lens was further adjusted by any required overrefraction needed to correct the habitual prescription. The simulated near images were viewed through the monofocal IOL with trial lens correction for the actual viewing distance (+0.75 D) and an overrefraction adjustment, when needed.

E. Simulation and Presentation of Multifocal Distance Images

The ratio of the multifocal distance OTF to the monofocal distance OTF was used to compute the simulated appearance of distance multifocal images (marked 0.0 D in Fig. 5). To obtain the more-blurred images, the multifocal distance OTF was measured at three levels of spectacle defocus (+0.5 D, +0.75 D, and +1.5 D), and the corresponding OTF ratios were computed by dividing the various defocus multifocal OTF's by the monofocal distance (in-focus) OTF. The +0.5-D-condition data was not used owing to insufficient sampling of the OTF for this condition. To obtain the sharper set of images, the monofocal distance OTF was measured at three levels of spectacle defocus (-0.125 D, -0.25 D and -0.5 D), and the corresponding OTF ratios were computed by dividing the multifocal distance OTF by the various out-of-focus monofocal OTF's. Note that the use of the defocused images represents an arbitrary way of creating blurrier and sharper images for comparison. However, this method provides us with a way of assessing the magnitude of the effect in terms of the familiar dioptric blur.

In this case, the subjects viewed the original unfiltered image through the multifocal IOL and the simulated image through the monofocal IOL. For both eyes a +0.75-D trial lens correcting for the actual viewing distance was used as well as an overrefraction adjustment, when needed.

As shown in Figs. 4 and 5, the filter functions were truncated to 1.0 if the filter exceeded 1.0. Although it is traditional to limit filter functions to values less than 1.0, there is nothing in Eq. (2) to restrict the filter function to 1.0 (if the multifocal lens can be designed and manufactured to have, at any frequency, a higher MTF than a monofocal lens; ours could not). The only filters that exceeded the value of 1.0 were those in which the multifocal lens MTF was divided by the MTF of a defocused monofocal lens. These filters represent an arbitrary (but con-

sistent) method of generating retinal images that were expected to be sharper than those generated by the multifocal lens. The restriction of these filters to 1.0 was aimed at reducing the probability of artifacts caused by the interaction of the high filter values with the limited dynamic range of the displayed images. Nevertheless, images generated with these truncated filters ended up at or close to the asymptotic value of the psychometric function, and thus the restriction had minimal effect on the results.

F. Data Analysis

The proportion of trials for which the simulated image (seen through the monofocal lens) was selected as being blurrier than the original image (seen through the multifocal lens) was plotted as a function of the simulated refractive error and was fitted with a psychometric function of the form

$$P = \text{norm}[(d - D)/s], \quad (3)$$

where $\text{norm}[\cdot]$ is the normal cumulative probability function, d is the simulated dioptric error, and D and s are the parameters of the fit representing the 50% transition point and the slope of the function, respectively. The computed value of D was used to indicate a simulated image that is indistinguishable from the standard image under the experimental viewing conditions. This value was recorded for each subject viewing each scene at both distances.

G. Liquid-Crystal Shutter Extinction and Fluorescent Persistence

In pilot experiments we found that the extinction factor of the LC shutters appeared insufficient. The image that is supposed to be invisible through one of the shutters was visible, although much dimmer than the other image. The effect does not represent a limited extinction of the ferro-electric LC stereo shutters but rather represents the persistence of the CRT display phosphor. At the high refresh rate used (122.5 Hz), the phosphor did not have sufficient time to decay from one image before the shutter reopened to let the other image through.

The display mean luminance without the LC shutters was 30 candelas per square meter (cd/m^2). When measured through the open shutter, it was reduced to $4.7 \text{ cd}/\text{m}^2$ (16%). The same mean luminance measured through the closed shutter was $0.4 \text{ cd}/\text{m}^2$ (1.3%). This results in a visible dim image instead of complete extinction. The visibility of the sharp original image seen with the monofocal eye, even when very dim, caused it to be fused with the image seen with the multifocal eye, which was optically blurred; as a result, the fused image appeared much sharper.

This effect was minimized or eliminated by replacing the images with a bright rather than a dark uniform background during the interval when they were not supposed to be seen. As a result, the decaying image was overwritten by a bright background, resulting in very low contrast for the residual, sufficient to make it virtually invisible. The only limitation of this solution is that the bright background attenuated by the shutters was superimposed on the bright image seen by either eye. This

caused both images to be presented at a slightly lower contrast than computed. The effect is small and applied to both images, and thus its impact on the results is expected to be minimal. In any case the problem of phosphor persistence should be considered and addressed in any studies using shutters for temporal multiplexing.

3. RESULTS

Most subjects required some refractive correction over their habitual distance spectacles. This correction was included in the LC goggles in addition to the lenses needed for optical distance simulation. None of the sub-

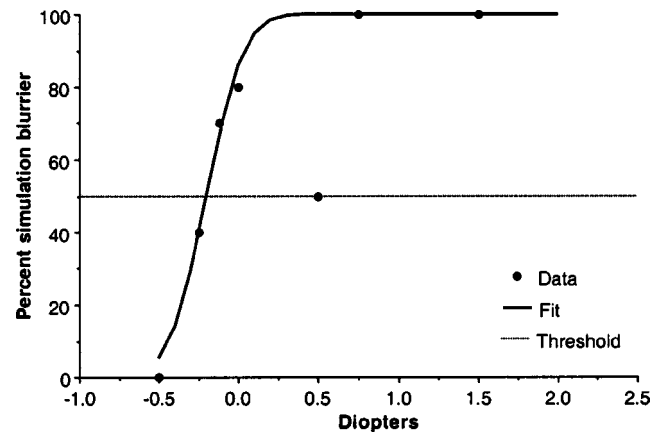


Fig. 6. Example of the data obtained for one subject (S4) at distance for the Boat image. Data points give the percent of the presentations in which the simulations were perceived blurrier than the image seen through the multifocal IOL. The fit represents a transition at 50% of -0.20 D as compared with a 0.0 D prediction. The image matching the original image seen through the multifocal IOL appeared slightly sharper than the 0.0 D prediction. The magnitude of the difference is very small; less than what would be caused by a 0.25-D error in the refraction. Note the point at 0.5 D that clearly deviates from the pattern of the rest of the data. This data point, the result of an erroneous filter, was not used in the fit.

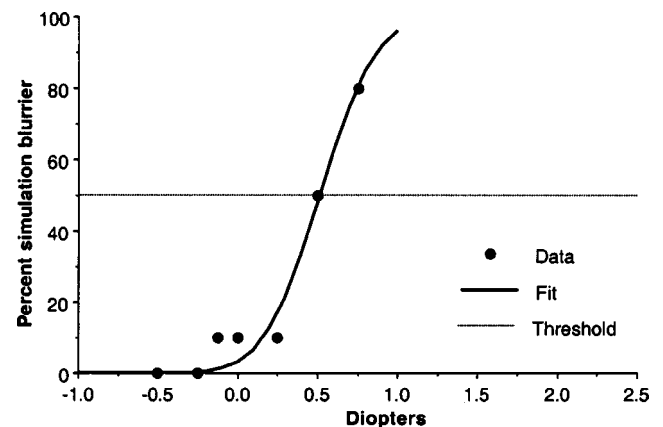


Fig. 7. Example of the data obtained for one subject (S3) at near distance for the Holly image. Data points give the percent of the presentations in which the simulations were perceived blurrier than the image seen through the multifocal IOL. The fit represents a transition at 50% of $+0.5 \text{ D}$ as compared with a 0.0 D prediction. The image matching the original image seen through the multifocal IOL is slightly blurrier than the 0.0 D prediction.

Table 1. 50% Transition Point for Each Subject and Image as Derived from the Curve Fitting to the Data^a

Image	Subject				Mean	Standard Deviation
	1	2	3	4		
Distance Vision Simulation (Prediction 0.0)						
Temple	-0.13	-0.21	0.02	-0.25	-0.14	0.12
Boat	-0.26	-0.36	0.15	-0.20	-0.17	0.22
Near Vision Simulation (Prediction 0.0)						
Chart	NA ^b	Eliminated	0.44	0.65	0.55	0.15
Plant	NA	0.75	0.52	0.06	0.44	0.35

^aA transition with a negative sign indicates that the image matching the original image seen through the multifocal IOL is sharper than the nominal or the predicted (0.0 D) image.

^bSubject 1 did not complete the near testing.

jects had any difficulty understanding the instructions and following them. No subject reported any difficulty seeing both images simultaneously during the experiment. All of the subjects could make appropriate and orderly selections of the sharper images, which were monotonically consistent with the simulated blur (Figs. 6 and 7). However, one subject (Subject 2 in Table 1) indicated that the simulated chart image was always blurrier than the original seen through the multifocal IOL. It was therefore impossible to fit the psychometric function, and that data point was eliminated from the analysis. There were usually two or three data points along the slope of the psychometric function, indicating that the steps of the simulations were sufficiently small and the simulations sufficiently close to the veridical appearance to provide sensitive testing. In Fig. 6 note the data point at +0.5 D that is farthest from the fit. The same deviation was noted in three of the four subjects' results. Further evaluation revealed an error in the filter applied to the corresponding images (discussed above). The detection of this error is another indication of the sensitivity and validity of the testing method. Removal of this point resulted in a very minor change of the results for one subject only (by 0.15 D) and no change for the others. Therefore data analysis did not include the responses to this condition.

The 50% transition point for each subject and average results are shown in Table 1. The average transition points found were similar for the two images in each of the two viewing conditions. For the distance-vision simulations, the subjects generally selected a slightly sharper simulated image than the nominal as matching the original image seen through the multifocal IOL. But the mean deviations (as well as those of individual subjects) from the prediction are equivalent to the small blur caused by less than 0.25-D error in refraction.

For the near testing, the average deviation from the prediction is slightly larger (approximately +0.5 D). In this case the subjects selected a more blurred image than the nominal as matching the original image seen through the near ADD of the multifocal lens. This could represent a slight error in the simulations or the effects of lens artifacts discussed below, which are more severe in the near testing because a higher-power trial lens is being used. It also should be noted that by design the multifocal distance image quality is superior to that at near; e.g.,

compare the 0.0-D filters in Figs. 4 and 5. The distance is weighted more to maintain distance image quality in low light and low contrast situations such as night driving.

4. DISCUSSION

The data from the distance testing indicate that the simulations corresponded well to the appearance of the images seen through the multifocal IOL. The consistency of the results with such a small number of elderly observers who were inexperienced with psychophysical testing demonstrates that the methods of simulation and testing were valid. In particular it is important to note that the differences in responses to the different scenes were not large and may be attributable to the subjects' use of specific details.

Thus the simulation of retinal images using this method may be a valid way to evaluate various multifocal IOL designs. Further, to the extent that the optics of a monofocal IOL lens is similar to that of the crystalline lens, the results suggest that such simulations may be used to illustrate to people with normal sight the appearance of various scenes with a specific multifocal lens design. Such use is limited in two ways. First, due to limitations in the electronic display's dynamic range, it is impossible to represent night scenes, and thus it is impossible to simulate the appearance of halos around bright lights and car-headlight glare that are reported to increase with multifocal lenses.¹ Second, candidates for such IOL's usually have cataracts in both eyes, and thus their retinal images will be affected by the cataracts when viewing such simulated images. Though compensation for the cataract effect may be possible, it has not been demonstrated yet.

Statistical power analysis based on the current data from the distance testing indicates that approximately 20 subjects would be required for a formal test of the validity of the simulated images. Given that this is not a recommended prescription mode, we are unlikely to recruit enough subjects with a monocular multifocal IOL in one eye and a monofocal IOL in the other eye in otherwise normal, disease-free eyes to achieve the required power.

The slightly larger deviation in the results from the prediction for the near testing is presumed to be a result

of the edge blur that occurs in the image seen through the multifocal IOL eye due to the high-power trial lens used. Although the simulation seen with the monofocal eye affects only the internal part of the image, the blurring lens used in front of the multifocal eye affects both the internal parts of the image and the border between the image and the blank background next to it. In addition to this effect, the minus lens induced significant magnification that may affect the perception of blur as well. These effects need to be further evaluated.

In conclusion, we have demonstrated that simulation of vision through an IOL is possible and may be veridical if the lens OTF and the OTF of the observer's eye can be reasonably estimated. Such simulations may serve as a design and analysis tool.

ACKNOWLEDGMENTS

This study was supported in part by Allergan Inc., by National Institutes of Health grants EY05957 and EY12890, and by Department of Energy Center for Excellence in Medicine grant DE-FG 02-91 ER61229. We thank Steve Lehar for help in data collection and Debra Trentacost for help in recruiting subjects.

Corresponding author Eli Peli can be reached at the address on the title page or by phone, 617-912-2597; fax, 617-912-0111; or e-mail, eli@vision.eri.harvard.edu.

REFERENCES AND NOTES

1. R. F. Steinert, B. L. Aker, D. J. Trentacost, P. J. Smith, and N. Tarantino, "A prospective comparative study of the AMO ARRAY zonal-progressive multifocal silicone intraocular lens and a monofocal intraocular lens," *Ophthalmology* **106**, 1243–1255 (1999).
2. J. C. Javitt, F. Wang, D. J. Trentacost, M. Rowe, and N. Tarantino, "Outcomes of cataract extraction with multifocal intraocular lens implantation: functional status and quality of life," *Ophthalmology* **104**, 589–599 (1997).
3. R. F. Steinert, "Visual outcomes with multifocal intraocular lenses," *Current Opinion in Ophthalmology* **11**, 12–41 (2000). Note: this review summarizes all recent publications on the ARRAY multifocal IOL, the only FDA-approved product, and summarizes current publications of other multifocal and bifocal IOL designs available primarily in Europe.
4. A. P. Ginsburg, "Visual information processing based on spatial filters constrained by biological data," Ph.D. dissertation (Cambridge University, Cambridge, UK, 1978).
5. B. L. Lundh, G. Derefeldt, S. Nyberg, and G. Lennerstrand, "Picture simulation of contrast sensitivity in organic and functional amblyopia," *Acta Ophthalmol.* **59**, 774–783 (1981).
6. E. Peli, "Contrast in complex images," *J. Opt. Soc. Am. A* **7**, 2032–2040 (1990).
7. L. N. Thibos and A. Bradley, "The limits of performance in central and peripheral vision," in Vol. 22 of *Digest of Technical Papers* (Society for Information Display, Santa Ana, Calif., 1991), pp. 301–303.
8. J. Larimer, "Designing tomorrow's displays," *NASA Tech. Briefs* **17**, 14–16 (1993).
9. J. Lubin, "A visual discrimination model for imaging system design and evaluation," in *Vision Models for Target Detection*, E. Peli, ed. (World Scientific, Singapore, 1995), Chap. 10, pp. 245–283.
10. J. T. Holladay, H. van Dijk, A. Lang, V. Portney, T. R. Willis, R. Sun, and H. C. Oksman, "Optical performance of multifocal intraocular lenses," *J. Cataract Refract. Surg.* **16**, 413–422 (1990); erratum, 781 (Nov. 1990).
11. R. Navarro, M. Ferro, P. Artal, and I. Miranda, "Modulation transfer functions of eyes implanted with intraocular lenses," *Appl. Opt.* **32**, 6359–6367 (1993).
12. E. Peli, L. Arend, and A. T. Labianca, "Contrast perception across changes in luminance and spatial frequency," *J. Opt. Soc. Am. A* **13**, 1953–1959 (1996).
13. E. Peli and G. Geri, "Testing the simulation of peripheral vision with image discrimination," in Vol. 30 of *Digest of Technical Papers* (Society for Information Display, Santa Ana, Calif., 1999), pp. 424–427.
14. V. Portney, "Optical testing and inspection methodology for modern intraocular lenses," *J. Cataract. Refract. Surg.* **18**, 607–613 (1992).
15. E. Peli, "Display nonlinearity in digital image processing for visual communications," *Opt. Eng.* **31**, 2374–2382 (1992).
16. D. Swift, S. Panish, and B. Hippensteel, "The use of the Vision Works® in visual psychophysical research," *Spatial Vis.* **10**, 471–477 (1997).
17. A. Lang, V. Lakshminarayanan, and V. Portney, "Phenomenological model for interpreting the clinical significance of the *in vitro* optical transfer function," *J. Opt. Soc. Am. A* **10**, 1600–1610 (1993).